

PACS numbers: 32.30.Jc; 32.50.+d; 32.80.Fb
DOI: 10.1070/QE2006v036n08ABEH013186

Selective visible and near-IR emission of Er_2O_3 excited by a 10.6-μm CO_2 laser

V.M. Marchenko

Abstract. **The results of video and spectral studies of intense selective visible and near-IR emission of Er_2O_3 powder excited by a 10.6-μm CO_2 laser are presented. The selective emission spectra in the range 460 – 1700 nm correspond to the Er^{3+} spectra observed upon cathode-, photo- and thermal excitations. Conversion of the CO_2-laser radiation into selective emission is attributed to the excitation of the $^4I_{13/2}$ energy levels by fluctuations of the local vibration amplitudes and up-conversion transitions to higher energy levels of Er^{3+}. Selective emission is applicable for visualisation and digital photo and video recording of laser radiation corresponding to the absorption spectra of oxide screens and conversion of heat into laser radiation upon resonance narrowband pumping of active media in the visible and IR spectral regions.**

Keywords: *up-conversion and laser radiation of Er^{3+}, selective emitters, spectroscopy, visualisation.*

1. The optical properties of crystals and glasses activated by Er^{3+} ions are being extensively studied and used in lasers, fibreoptic and optoelectronic telecommunication devices, sensors [1 – 11], as well as in selective emitters (SEs) of thermal photovoltaic (TPV) generators [12 – 14]. Of considerable interest is the up-conversion of the population of Er^{3+} energy levels caused by resonance cross-relaxation transitions between the excited states of the screened shell of the $4f^{11}$ electron configuration [1 – 3, 6, 7, 9, 11]. Up-conversion of radiation at wavelengths ~ 0.8, 1 and 1.5 μm into the Er^{3+} luminescence in the visible spectral region is one of the methods for visualisation of the near-IR radiation.

Popular methods of visualising radiation in the mid-IR spectral region are thermal vision (thermography) and thermal quenching of luminescent screens [15, 16]. High-sensitivity thermal vision devices based on semiconductor or bolometric arrays, whose aperture (~ 1 cm) is limited by the number of pixels of size ~ 20 μm, are used in spectral regions of 5 and 10 μm. Visualisation of larger apertures (more than 10 cm) of IR radiation wave fronts is performed by the method of thermal quenching of luminescence of ZnS, CdS, etc. excited by UV radiation, resulting in the formation of a negative image on film screens.

Refractory oxides of rare earths are characterised by not continuous but selective thermal emission spectra [17 – 19], which are efficiently used in selective emitters of TPV generators [12 – 14]. The temperature dependence of the spectral emissivity of incandescent Er_2O_3 powder was studied in [17, 18] in the temperature range 873 – 1493 K. At Er_2O_3 temperatures exceeding 873 K, broad spectral lines were observed in blue, green and red regions with intensity at 1273 K several times higher than that of the blackbody radiation at the same temperature [17, 18]. In [18], this was attributed to additional luminescence caused by thermal transformation of chemical and/or physical properties of the powder. According to [19], however, the spectral emissivity of pellets pressed from the Er_2O_3 powder was lower than 0.6 in the visible and near IR spectral regions in the temperature range 1540 – 1873 K.

2. In this paper, we present the results of experimental investigations of intense visible and near-IR selective emission of the microcrystalline Er_2O_3 powder excited by a ~ 100-W electric-discharge cw CO_2 laser at 10.6 μm and consider the possibility of using the powder for visualising laser radiation in the mid IR spectral region and for resonance excitation of laser-active media.

In our experiments, the laser beam was directed at a loose or slightly rammed ~ 1-mm thick layer of a microcrystalline Er_2O_3 powder on a silicon substrate. The characteristic size of microcrystalline particles was 5 – 30 μm. The average laser power was set by a shutter, and the radiation intensity – by focusing by an NaCl lens. The radiation intensity at the powder surface did not exceed 2.5 kW cm^{-2} at an average power of 3.6 W. The temperature in the layer was measured with the help of a chromel – alumel thermocouple and did not exceed 1573 K.

The emission of the Er_2O_3 powder was photographed with a MITO E323A digital video camera with a resolution of 1280 × 1024 pixels. Figure 1 shows the laser spot of a multimode CO_2 laser on the screen in the form of an Er_2O_3 powder layer. The emission spectrum of samples in the range 200 – 1100 nm was recorded with an AvaSpec-2048 (Avantes) fibreoptic diffraction spectrometer having the spectral resolution of the diode array equal to 0.8 nm. The spectral sensitivity of the spectrometer was calibrated by an incandescent tungsten lamp with the brightness temperature of 2854 K. The fibreoptic input to the spectrometer was aligned at a small angle to the laser beam at a distance of ~ 9 cm from the sample surface. Figure 2a

V.M. Marchenko A.M. Prokhorov General Physics Institute, Russian Academy of Sciences, ul. Vavilova 38, 119991 Moscow, Russia; e-mail: vmarch@kapella.gpi.ru

Received 30 March 2006
Kvantovaya Elektronika **36** (8) 727 – 730 (2006)
Translated by Ram Wadhwa

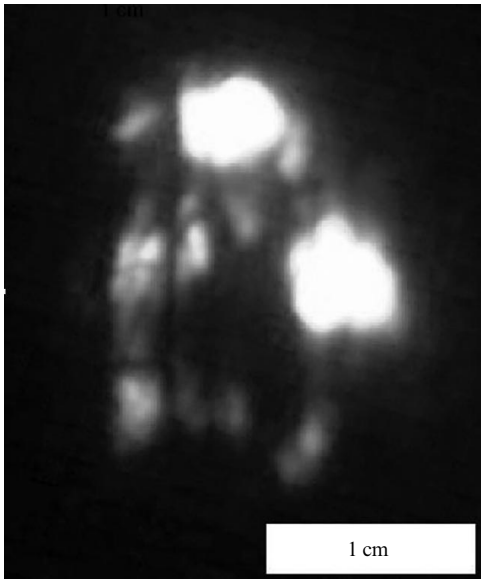

Figure 1. Selective emission on a screen formed by a layer of Er_2O_3 powder excited by a ~ 100-W multimode CO_2 laser at 10.6 μm.

shows the normalised selective emission spectrum of the Er_2O_3 powder at a temperature of ~ 1273 K in the spectral range 350 – 1100 nm. The noise in the spectrum was suppressed by averaging over 20 points. Figure 2b shows the selective emission spectrum of the Er_2O_3 powder in the spectral range 1100 – 1700 nm at the same temperature, recorded with a NIR128-1.7-RS232 (Avantes) fibreoptic diffraction spectrometer equipped with an InGaAs detector array with a flat spectral sensitivity.

Table 1 presents the wavelengths of broad emission lines of the Er_2O_3 powder excited by a 10.6-μm CO_2 laser. The selective emission spectrum of the Er_2O_3 powder is anti-Stokes with respect to the excitation line. Its selectivity in the case of excitation by a CO_2 laser is attributed to transitions from the excited electronic states of the screened $4f^{11}$ shell of trivalent Er^{3+} ions to the ground $^4I_{15/2}$ state [1, 4, 7, 19]. The line selective emission spectrum in the range 460 – 1700 nm observed upon excitation by a CO_2 laser corresponds to the known spectra of Er_2O_3 powders obtained upon cathode-, photo- or thermal excitation. It must be noted in this case that for the temperature range 10 – 1873 K, the relative intensity of the $^4I_{13/2} \rightarrow {}^4I_{15/2}$ transitions in the spectral range 1200 – 1600 nm has a weaker dependence on the excitation method and temperature than the intensity of short-wavelength spectral lines [3, 4, 19]. The smaller width of up-conversion lines of

Table 1. Interpretation of selective emission spectrum of the Er_2O_3 powder excited by a 10.6-μm CO_2 laser.

Wavelength of the selective emission band of Er_2O_3/nm	Upper levels of transitions to the $^4I_{15/2}$ ground state of Er^{3+}
460	$^4F_{5/2}$
490	$^4F_{7/2}$
540	$^2H_{11/2}$
560	$^4S_{3/2}$
665	$^4F_{9/2}$
805	$^4I_{9/2}$
980, 1010	$^4I_{11/2}$
1475, 1545	$^4I_{13/2}$

luminescence spectra compared to the Stokes luminescence spectra of Er^{3+} [3, 5, 6, 9, 11] is obviously explained by resonance laser pumping.

Under the conditions of thermodynamic equilibrium, the ratio of the selective emission line intensities to the intensity of blackbody radiation determines the spectral dependence of the emissivity or greyness of Er_2O_3.

The increase in the relative band intensity of selective emission of Er_2O_3 powder with wavelength in the spectral region 400 – 985 nm was interpolated by the blackbody radiation spectra [curves (*2* – *4*) in Fig. 2]. The interpolation was not extended to the entire spectral range 400 – 1700 nm because of mismatching of spectral sensitivity of the spectrometers. Because radiation was detected with the diode array, the curves for the blackbody radiation spectra were calculated from Planck's formula for photon distribution

$$P(\lambda, T) \sim \left[\lambda^4 \left(\exp\frac{hc}{\lambda kT} - 1\right)\right]^{-1},$$

where h is Planck's constant; k is the Boltzmann constant; and c is the velocity of light [20]. The interpolation curves were normalised to the maximum intensity of the 980 nm ($^4I_{11/2} \rightarrow {}^4I_{15/2}$) spectral line at temperatures 1300, 1700 and 2000 K. For the temperature of the Er_2O_3 powder equal to 1300 K measured by a thermocouple, the 805-nm ($^4I_{9/2} \rightarrow {}^4I_{15/2}$), 665-nm ($^4F_{9/2} \rightarrow {}^4I_{15/2}$) and 560-nm ($^4S_{3/2} \rightarrow {}^4I_{15/2}$) spectral lines are located higher than interpolation curve (*2*) (see Fig. 2), i.e., they correspond to a higher temperature. At $T = 1700$ K, the interpolation curve touches the peaks of the 980-nm and 805-nm spectral lines with close (~ 100 s^{-1}) probabilities of spontaneous radiative transitions, but 'intersects' the 665-nm and 560-nm lines. At $T = 2000$ K, the interpolation curve touches the peaks of the 980-nm and 560-nm spectral lines and passes above the remaining lines. The interpolation temperatures were found to be much higher than the experimentally measured temperatures of the Er_2O_3 powder (less than 1573 K). This fact does not contradict to the observation of nonequilibrium selective emission of Er_2O_3 reported in [17, 18], with the spectral line intensities in blue, green and red spectral regions in the temperature interval 1213 – 1313 K higher than the intensity of blackbody radiation.

3. The conversion of thermal energy into selective emission of rare-earth ions was studied theoretically, mainly to describe the TPV processes [21, 22]. According to the models proposed in these papers, selective emission appears due to radiative transitions in the screened electron shell of ions with the 4f configuartion. It was assumed that non-radiative excitation of electronic states occurs due to perturbation of the electron shell caused by the thermal shift of charges upon electron – phonon interaction [22]. As the temperature increases under equilibrium conditions, the relative intensity of the selective radiation lines must correspond to the Boltzmann population of electronic levels. However, the measured temperature dependence of the spectral emissivity of pellets made of the Er_2O_3 powder in the temperature range 873 – 1873 K [17 – 19], an increase in the relative intensity of short-wavelength selective emission lines with temperature [19], as well as the interpolation of spectra in the present paper, all point towards a violation of the equilibrium conditions.

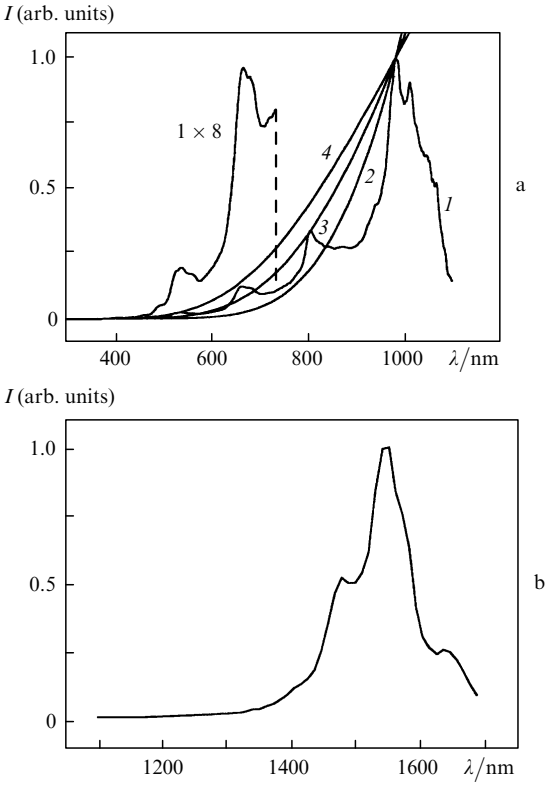

Figure 2. (a) Selective emission spectra of the Er_2O_3 powder excited by a 10.6-μm CO_2 laser in the spectral region 300 – 1100 nm [curve (*1*)] and short-wavelength tails of the normalised Planck's function at a temperature of 1300 K [curve (*2*)], 1700 K [curve (*3*)], and 2000 K [curve (*4*)] (1×8: the intensity is magnified by eight times). (b) Emission spectrum in the region 1100 – 1700 nm.

Let us analyse the mechanism of conversion of laser radiation at a wavelength of 10.6 μm into selective emission of Er^{3+} ions in the visible and near-IR spectral regions. We will consider the possible processes of excitation of electronic levels of Er^{3+} by CO_2-laser radiation. The energy of IR photons (~ 0.12 eV, $\lambda = 10.6$ μm) is lower than the energy of the $^4I_{13/2}$ level (~ 0.8 eV, $\lambda = 1.55$ μm), and the probability of multiphoton $^4I_{15/2} \rightarrow {}^4I_{13/2}$ transitions is low for the given intensity of laser radiation. Laser radiation at 10.6 μm was localised at the Er_2O_3 powder. The intrinsic absorption of the CO_2 laser radiation by the Er_2O_3 crystal matrix leads to a heating of the samples. The spectral emissivity of the garnet $Er_3Al_3O_{12}$ is continual (~ 0.8) in the region 5.3 – 10 μm [12]. In the above temperature range, the thermal energy in the microcrystalline Er_2O_3 powder is mainly concentrated in the vibrational degrees of freedom. It is reasonable to assume that thermal excitation of phonons is the main source of excitation of the $^4I_{13/2}$ energy levels. Most probably, excitation by IR radiation triggers the multiphoton fluctuation mechanism of excitation of $^4I_{13/2}$ levels in a manner analogous to the diffusion mechanism in crystals when the phonon energy (less than 0.25 eV in the present case) is lower than the height of the potential barrier [23]. In an elementary act, the potential energy achieves the excitation energy of the $^4I_{13/2}$ level if the equilibrium ion shifts are locally exceeded due to the random phase synchronisation of normal vibrations.

The subsequent cooperative interaction of excited electronic states of Er^{3+} ions and cross relaxation are accompanied by up-conversion electronic transitions [1 – 3, 5, 7, 9, 11]

$$^4I_{13/2}(0.8\ \text{eV}) + {}^4I_{13/2}(0.8\ \text{eV}) \rightarrow {}^4I_{9/2}(1.55\ \text{eV}) + {}^4I_{15/2},$$

$$^4I_{11/2}(1.27\ \text{eV}) + {}^4I_{11/2}(1.27\ \text{eV}) \rightarrow {}^4S_{3/2}(2.22\ \text{eV}) + {}^4I_{15/2},$$

$$^4I_{11/2}(1.27\ \text{eV}) + {}^4I_{11/2}(1.27\ \text{eV}) \rightarrow {}^4H_{11/2}(2.31\ \text{eV}) + {}^4I_{15/2}$$

leading to the population of higher states from which luminescence in the visible spectral region is observed.

The above temperature dependence of the intensity of short-wavelength thermal radiation lines from Er_2O_3 powder points towards the up-conversion mechanism of selective emission of Er_2O_3 [19]. An indirect confirmation of such a mechanism of selective emission of Er_2O_3 is provided by the low probability of nonradiative relaxation of the first excited $^4I_{13/2}$ electronic state in erbium-doped glasses at relatively low temperatures. For a typical lifetime of $\sim 5 - 10$ ms for the $^4I_{13/2}$ level at room temperature [24], this probability is two orders of magnitude lower than the probability of radiative transition to the ground $^4I_{15/2}$ state or is comparable with it. The population N of the $^4I_{13/2}$ levels is determined under equilibrium conditions by the factor $N(^4I_{13/2})/N(^4I_{15/2}) = \exp(-hc/\lambda kT)$. The population $N(^4I_{13/2}) \approx 1.7 \times 10^{19}$ cm^{-3} in microcrystalline Er_2O_3 at $T = 1300$ K is comparable with the population of these levels in the case of resonance laser excitation of the up-conversion luminescence in doped materials. The temperature flare of selective emission [18] is explained qualitatively by an increase in the intensity of up-conversion luminescence lines upon an increase in $N(^4I_{13/2})$ with temperature due to a rise in the fluctuation density at the initial stage of heating and the competing process of luminescence quenching at higher temperatures. According to the thermodynamic model of selective emitters [21], conversion of heat into selective emission may lead to nonequilibrium conditions due to radiation-induced cooling of excited states of erbium ions.

4. An analysis of the known spectral studies as well as those carried out in this work explains the mechanism of conversion of laser radiation in the mid IR range into selective emission of Er_2O_3 in the visible and near IR spectral regions, as well as its temperature dependence. We have paid attention to the role of up-conversion excitation of short-wavelength selective emission lines. The use of selective emission of rare-earth oxides opens new possibilities for visualisation, digital photo- and video recording of intensity distributions on wide-aperture screens and broadens the range of application of laser spectrometry and interferometry. The spectral sensitivity range of the screens is determined by the absorption spectra of oxide layers and the substrate material. The image contrast depends on the structure of oxide screens and temperature gradients in the emitting layer.

The efficiency of a SE is determined by the ratio of the energy flux of oxide layer radiation in the visible and near IR spectral regions to the heat fluxes in the heater with thermal losses, including thermal radiation to the environment. The ratio of the useful radiation energy for the TPV generators to the total radiant energy from the SE achieves ~ 40 %, while the conversion coefficient of thermal energy

into electric energy is $\sim 10\,\%$ [12, 13]. High-efficiency SEs based on rare-earth oxides are of considerable interest as converters of thermal energy into resonance narrowband selective pump radiation for laser-active media in the visible and IR spectral regions. Selective emission of Er_2O_3 is in resonance with the electronic levels of erbium lasers. The high-intensity spectral line of selective emission from Yb_2O_3 at the wavelengths $0.9-1.1$ μm of the $^2F_{5/2} \rightarrow {}^2F_{7/2}$ transition of Yb^{3+} ions corresponds to the $^4I_{15/2} \rightarrow {}^4I_{11/2}$ absorption lines of Er^{3+} ions [19]. Oxide-mixture-based SEs with a broadband spectrum in the visible region are also of practical interest.

Acknowledgements. The authors thank K.N. Firsov, V.A. Yur'ev, V.V. Smirnov, and V.I. Fabelinskii for useful discussions, V.M. Borozdov for his help in the experiments, and M.G. Voitik and A.L. Tomashuk for their assistance in spectral investigations.

References

1. Bagdasarov Kh.S., Zhekov V.I., Lobachev V.A., et al. *Trudy IOFAN*, **19** (5), 5 (1989).
2. Van der Ziel J.P., Ostermayer F.W., Van Uitert L.G. *Phys. Rev. B*, **2**, 4432 (1970).
3. Jaba N., Kanoun A., Mejri H., et al. *J. Phys.: Condens. Matter*, **12**, 4523 (2000).
4. Plugaru R., Piqueras J., Nogales E., et al. *J. Optoelectron. Adv. Mater.*, **4**, 8834 (2002).
5. Lin H., Jiang S., Wu J., et al. *J. Phys. D: Appl. Phys.*, **36**, 812 (2003).
6. Seat H.C., Sharp J.H. *Meas. Sci. Technol.*, **14**, 279 (2003).
7. Kik P.G., Polman A. *J. Appl. Phys.*, **93**, 5008 (2003).
8. Lira A., Camarillo I., Camarillo E., et al. *J. Phys.: Condens. Matter*, **16**, 5925 (2004).
9. Diaz-Torres A., De la Rosa-Cruz E., Salas P., Angeles-Chavez C. *J. Phys. D: Appl. Phys.*, **37**, 2489 (2004).
10. Fujii M., Imakita K., Watanabe K., Hayashi S. *J. Appl. Phys.*, **95**, 272 (2004).
11. Yang Z., Xu S., Hu L., Jiang Z. *J. Mater. Sci.*, **39**, 2223 (2004).
12. Chubb D.L., Pal A-M.T., Patton M.O., Jenkins P.P. *J. Eur. Ceram. Soc.*, **19**, 2551 (1999).
13. Bitnar B., Durisch W., Mayor J.-C., et al. *Solar Energy Mater. Solar Cells*, **73**, 221 (2002).
14. Licciulli A., Diso D., Torsello G., et al. *Semicond. Sci. Technol.*, **18**, S174 (2003).
15. Bazhulin A.P., Irisova N.A., Sasorov V.P. *Vestnik Akad. Nauk SSSR*, **12**, 15 (1973).
16. Zaitsev L.M., Klyuchnikov V.M., Sonin A.S., et al. *Kvantovaya Elektron.*, **4**, 1351 (1977) [*Sov. J. Quantum Electron.*, **7**, 761 (1977)].
17. Mallory W.S. *Phys Rev.*, **14**, 54 (1919).
18. Nichols E.L., Howes H.L. *Phys. Rev.*, **19**, 300 (1922).
19. Guazzoni G.E. *Appl. Spectroscopy*, **26**, 60 (1972).
20. Kikoin I.K. *Tablitsy fizicheskikh velichin* (Tables of Physical Quantities) (Moscow: Atomizdat, 1976).
21. Golovlev V.V., Winston Chen C.H., Garrett W.R. *Appl. Phys. Letts.*, **69**, 280 (1996).
22. Torsello G., Lomascolo M., Licciulli A., et al. *Nature Mater.*, **3**, 632 (2004).
23. Boltaks B.I. *Diffusion in Semiconductors* (New York: Acad. Press, 1963; Moscow: Fizmatgiz, 1961).
24. Yang J., Dai S., Dai N., et al. *J. Lumin.*, **106**, 9 (2004).